Orbit Determination for Asteroid 214088 (2004 JN13) Using Gauss' Method

Chunyang Ding, Hannah Nikole Almonte, and Joan Creus Costa

Summer Science Program 2014, Santa Barbara, California.

July 26, 2014

Asteroid orbit determination is crucial for predicting potentially cataclysmic events, as well as increasing the understanding of our solar system. This paper studies the Near Earth Asteroid 214088 (2004 JN13) through five observations spread throughout June and July of 2014. By processing CCD images with the Least Squares Plate Reduction, the right ascension and declination of the asteroid at various timestamps were determined. This data was then processed using the Method of Gauss to determine the classical orbital elements, obtaining $a = 2.9136 \pm 0.2046$, $e = 0.7007 \pm 0.0227$, $i = 13.4179^\circ \pm 0.7980^\circ$, $\Omega = 88.3553^\circ \pm 0.4534^\circ$, $\omega = 275.9211^\circ \pm 1.4043^\circ$ and $T = 2455122 \pm 193$). The uncertainties in the orbital elements were calculated using the Monte Carlo method, and were checked by generating ephemeris data for days in which the asteroid was measured and comparing with the observed values. The expected and observed values were found to be within the expected range of error.

1. Introduction

Orbit determination of asteroids is necessary to enhance public databases for the purposes of predicting near-earth asteroids that are potentially hazardous to the planet. Today, astronomers use methods to calculate the long term orbit of asteroids with high confidence, given sufficient observations. This paper discusses the orbit of Asteroid 214088 (2004 JN13) as calculated through Gauss's method. Data was collected via multiple observations of the asteroid in Santa Barbara, CA and La Serena, Chile. In order to check for uncertainty, a Monte Carlo simulation was used, and the resulting orbit was matched against other collected data.

In 1809, numerical integration as a method of orbit determination was devised by Carl Friedrich Gauss to predict the location of Asteroid 1 Ceres for further observa-

tions.[1] His method uses Newtonian gravity, vector geometry, and differential calculus to approximate orbits. His method is still used by modern astronomers to determine orbits of asteroids.

Upon completion of the Initial Orbit Determination (IOD), a simulation of the IOD was used to examine the accuracy of our results. In addition, the simulation models the orbit to check if the asteroid poses danger to Earth. By assuming a Gaussian distribution for the data, the Monte Carlo method of simulations determined the uncertainty values for the calculated orbital elements.

2. Methods

2.1. Data collection

To obtain data, we used three different telescopes: the 24-inch Keck and 14-inch Meade telescopes at Westmont College in Santa Barbara, CA, and the 0.4-meter Prompt1 telescope at Cerro Tololo Inter-American Observatory (CTIO) in La Serena, Chile. During observations, the team used software such as TheSkyX[2] and CCDSoft to take 30 to 45 second exposures of our asteroid. After observations, sets of 3 to 5 observations were median combined using MaxImDL software. These images were processed using Python programs to determine the Right Ascension (α) and Declination (δ) of the asteroid.

A consistent procedural problem we encounter involves the SkyX Epoch at the Keck. It was not set to Epoch J2000, which is the Epoch that the JPL Horizons website uses. As a result, observing teams have to manually change the Epoch in order to slew the telescope to the correct field of view. Despite this difficulty, data from the images were still obtained.

2.2. Data processing

The nature of Gauss's method of orbital determination requires numerous iterative steps and the processing of large data sets, favoring automatized programs over hand calculations. A function known as the plate scale was written to convert xy coordinates of images to $\alpha\delta$ coordinates of the asteroid. This plate scale was derived by matching the centroids of eight or more stars on each image to reference stars of known $\alpha\delta$ taken from the UCAC3 catalog. The centroid program determines the center of stars and asteroids by calculating the weighted average of photon counts per pixel. The Least Square Plate Reduction(LSPR) program reads an image and constructs a linear regression to construct the plate scale.These two programs combined results in equations of the form:

$$\alpha = b_1 + a_{11}x + a_{12}y \tag{1}$$

$$\delta = b_2 + a_{21}x + a_{22}y \tag{2}$$

where $a_11, a_12, a_21, a_22, b_1, b_2$ are constants determined by the LSPR program. The σ_α and σ_δ, were also calculated (Table 1).

As seen in Fig 1, vector geometry between the Sun-Earth-Asteroid system allows for the equation:

$$\hat{\mathbf{r}} = \rho\hat{\rho} - \hat{\mathbf{R}} \tag{3}$$

to be valid for all cases, where the $\hat{\rho}$ is determined by the RA/DEC of the asteroid, and the parallax corrected $\hat{\boldsymbol{R}}$ is taken from the JPL HORIZONS database. Therefore, if the distance from the Earth to the asteroid is known, then the equatorial position, $\boldsymbol{r}$, of the asteroid can be calculated.

[1] Marsden 1977.
[2] Bisque 2014.

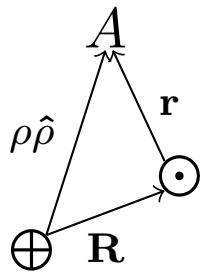

Figure 1: Diagram of the Earth, Sun and asteroid positions.

There are several methods for calculating the ρ distance, including parallax or radio astronomy.[3] However, given the resources available, we approximate ρ through f and g series. This approximation allows for a better estimate of $\boldsymbol{r}$ and $\|\boldsymbol{r}\|$, which could then be used to once again calculate ρ. In addition, proper time (τ) is recalculated to correct for the travel time of light. Through iteration, the method converges to a true value of $\boldsymbol{r}$. The iterations terminate when the calculated value for ρ converges[4].

These equatorial position and velocity vectors are used to evaluate the classical orbital elements, as well as the Mean Anomaly, an element that is proportional to the area swept by the asteroid's orbit, and Perihelion Time, the time where the asteroid comes closest to the sun.[5] [6].

2.3. Error analysis

All errors in data collection were assumed to arise from LSPR calculation uncertainties; CCD uncertainties, centroid processing errors, and statistical anomalies would have been accounted for in the σ_α and σ_δ calculations. However, perturbation effects, rotation of the asteroid, and approximation errors are not accounted for in the simplified Kepler's equations, and thus the errors associated with these processes cannot be determined. Other papers published such as Binz et. al[7] and Gronchi[8] use other methods of determining uncertainty regions for the asteroid, but similar to Hussein et. al,[9] we choose to use the Monte Carlo method.

It is unreasonable to propagate error in an iterative algorithm such as in the method of Gauss. Therefore, the team elected to use the Monte Carlo method to calculate uncertainty. Given the known uncertainties in the α and δ for each of the observations, a normal distribution was assumed and sampling of a large number of values ($n = 1000$) was performed following that normal distribution. For each of the sampled right ascension and declination, the orbital elements were slightly different; the final value which was reported was the mean value for each element and the associated uncertainty was the standard deviation of the values for this element.

3. Results

3.1. Observations

The observed positions of the asteroid for each of the observations can be found in table 1. Each table includes the final measurements for right ascension and declination and the residuals of the reference stars the LSPR was performed with. The images whence this data comes from are in figure 2.

[3] JPL 2014.

[4] in this case, until subsequent values differ by less than 10^{-10}.

[5] Danby 1992.

[6] Full equations for this process can be found in the appendix

[7] Binz and Healy 2014.

[8] Gronchi 2004.

[9] Hussein et al. n.d.

2014/06/27 06:39:41.31 UT (JD 2456835.777562)

$\boldsymbol{\alpha = 246.124787^h}$ $\boldsymbol{(16^h24^m29.95)}$	$c_x = 211.288$
$\boldsymbol{\delta = -19.062\,028^\circ}$ $\boldsymbol{(-19^\circ3'43.30'')}$	$c_y = 277.263$

Stars used in the least squares fit:

$r_\alpha = 1.604\,36 \times 10^{-5}$	$r_\delta = -1.532\,28 \times 10^{-5}$	$\alpha = 246.233\,134^\circ$	$\delta = -19.147\,911^\circ$
$r_\alpha = 4.400\,36 \times 10^{-5}$	$r_\delta = 1.510\,63 \times 10^{-5}$	$\alpha = 246.139\,164^\circ$	$\delta = -19.180\,209^\circ$
$r_\alpha = -1.460\,53 \times 10^{-5}$	$r_\delta = -2.236\,71 \times 10^{-5}$	$\alpha = 246.048\,225^\circ$	$\delta = -18.952\,217^\circ$
$r_\alpha = 3.014\,61 \times 10^{-5}$	$r_\delta = -1.697\,52 \times 10^{-5}$	$\alpha = 246.105\,055^\circ$	$\delta = -18.935\,964^\circ$
$r_\alpha = 5.298\,51 \times 10^{-6}$	$r_\delta = -2.818\,82 \times 10^{-5}$	$\alpha = 246.005\,785^\circ$	$\delta = -19.033\,960^\circ$
$r_\alpha = -5.373\,93 \times 10^{-5}$	$r_\delta = 6.838\,01 \times 10^{-6}$	$\alpha = 245.971\,947^\circ$	$\delta = -19.049\,637^\circ$
$r_\alpha = -6.124\,74 \times 10^{-5}$	$r_\delta = -1.945\,91 \times 10^{-5}$	$\alpha = 246.189\,565^\circ$	$\delta = -19.025\,833^\circ$
$r_\alpha = -8.743\,93 \times 10^{-5}$	$r_\delta = -9.458\,23 \times 10^{-6}$	$\alpha = 246.225\,289^\circ$	$\delta = -19.066\,220^\circ$
$r_\alpha = 7.210\,62 \times 10^{-5}$	$r_\delta = 4.351\,74 \times 10^{-5}$	$\alpha = 246.243\,516^\circ$	$\delta = -19.066\,763^\circ$
$r_\alpha = 4.943\,33 \times 10^{-5}$	$r_\delta = 4.630\,91 \times 10^{-5}$	$\alpha = 245.998\,197^\circ$	$\delta = -18.918\,444^\circ$

Final α and δ fit

$$\alpha = 246.253\,573\,917 + -0.000\,590\,444\,656\,645x + -1.454\,561\,902\,06 \times 10^{-5}y$$
$$\delta = -18.910\,072\,600\,1 + 1.368\,005\,718\,57 \times 10^{-5}x + -0.000\,558\,479\,218\,063y$$

2014/07/02 07:13:55.00 UT (JD 2456840.801331)

$\boldsymbol{\alpha = 243.402163^h}$ $\boldsymbol{(16^h13^m36.52)}$	$c_x = 474.054$
$\boldsymbol{\delta = -19.794\,642^\circ}$ $\boldsymbol{(-19^\circ47'40.71'')}$	$c_y = 516.701$

Stars used in the least squares fit:

$r_\alpha = -7.573\,88 \times 10^{-7}$	$r_\delta = -1.229\,50 \times 10^{-4}$	$\alpha = 243.450\,125^\circ$	$\delta = -19.722\,106^\circ$
$r_\alpha = -1.169\,61 \times 10^{-5}$	$r_\delta = 2.264\,03 \times 10^{-4}$	$\alpha = 243.459\,833^\circ$	$\delta = -19.758\,208^\circ$
$r_\alpha = 1.781\,96 \times 10^{-5}$	$r_\delta = -1.696\,45 \times 10^{-5}$	$\alpha = 243.410\,208^\circ$	$\delta = -19.803\,228^\circ$
$r_\alpha = 3.373\,30 \times 10^{-5}$	$r_\delta = 1.377\,51 \times 10^{-5}$	$\alpha = 243.333\,250^\circ$	$\delta = -19.807\,981^\circ$
$r_\alpha = -2.145\,92 \times 10^{-5}$	$r_\delta = -6.752\,83 \times 10^{-5}$	$\alpha = 243.439\,958^\circ$	$\delta = -19.825\,536^\circ$
$r_\alpha = 2.707\,29 \times 10^{-5}$	$r_\delta = -6.532\,76 \times 10^{-5}$	$\alpha = 243.436\,292^\circ$	$\delta = -19.789\,886^\circ$
$r_\alpha = -1.858\,18 \times 10^{-5}$	$r_\delta = 3.273\,42 \times 10^{-5}$	$\alpha = 243.362\,250^\circ$	$\delta = -19.824\,875^\circ$
$r_\alpha = -2.613\,09 \times 10^{-5}$	$r_\delta = -1.414\,78 \times 10^{-7}$	$\alpha = 243.324\,042^\circ$	$\delta = -19.784\,203^\circ$

Final α and δ fit

$$\alpha = 243.486\,416\,495 + -0.000\,166\,634\,882\,907x + -1.017\,843\,583\,81 \times 10^{-5}y$$
$$\delta = -19.718\,155\,143\,9 + 9.592\,042\,801\,16 \times 10^{-6}x + -0.000\,156\,829\,183\,681y$$

2014/07/05 06:53:11.59 UT (JD 2456843.786940)

$\boldsymbol{\alpha = 242.350986^h}$ $\boldsymbol{(16^h09^m24.24)}$	$c_x = 330.499$
$\boldsymbol{\delta = -20.105\,582^\circ}$ $\boldsymbol{(-20^\circ6'20.10'')}$	$c_y = 246.078$

Stars used in the least squares fit:

$r_\alpha = 1.723\,68 \times 10^{-4}$	$r_\delta = 7.682\,40 \times 10^{-5}$	$\alpha = 242.398\,069^\circ$	$\delta = -20.057\,063^\circ$
$r_\alpha = -1.446\,97 \times 10^{-5}$	$r_\delta = -1.907\,17 \times 10^{-5}$	$\alpha = 242.334\,224^\circ$	$\delta = -20.080\,328^\circ$
$r_\alpha = -6.989\,81 \times 10^{-5}$	$r_\delta = 1.639\,18 \times 10^{-5}$	$\alpha = 242.306\,568^\circ$	$\delta = -20.105\,898^\circ$
$r_\alpha = -7.202\,90 \times 10^{-5}$	$r_\delta = -1.335\,70 \times 10^{-5}$	$\alpha = 242.270\,487^\circ$	$\delta = -20.156\,661^\circ$
$r_\alpha = 1.192\,22 \times 10^{-4}$	$r_\delta = -1.418\,19 \times 10^{-5}$	$\alpha = 242.366\,637^\circ$	$\delta = -20.140\,225^\circ$
$r_\alpha = -1.117\,86 \times 10^{-4}$	$r_\delta = -3.419\,33 \times 10^{-5}$	$\alpha = 242.517\,272^\circ$	$\delta = -20.042\,291^\circ$
$r_\alpha = -7.637\,55 \times 10^{-5}$	$r_\delta = 2.647\,65 \times 10^{-5}$	$\alpha = 242.307\,228^\circ$	$\delta = -20.017\,946^\circ$
$r_\alpha = 5.296\,74 \times 10^{-5}$	$r_\delta = -3.888\,83 \times 10^{-5}$	$\alpha = 242.279\,142^\circ$	$\delta = -19.988\,322^\circ$

Final α and δ fit

$$\alpha = 242.532\,317\,085 + -0.000\,591\,049\,612\,238x + 5.693\,587\,773\,63 \times 10^{-5}y$$
$$\delta = -19.951\,040\,447\,4 + -5.408\,782\,458\,24 \times 10^{-5}x + -0.000\,555\,375\,965\,969y$$

Table 1: Table of observations

2014/07/11 06:46:41.38 UT (JD 2456849.782423)

$\boldsymbol{\alpha = 238.833991^h}$ $\boldsymbol{(15^h55^m20.16)}$	$c_x = 359.315$
$\boldsymbol{\delta = -21.258\,265^\circ}$ $\boldsymbol{(-21^\circ15'29.75'')}$	$c_y = 229.380$

Stars used in the least squares fit:

$r_\alpha = 5.828\,41 \times 10^{-5}$	$r_\delta = 1.181\,34 \times 10^{-5}$	$\alpha = 238.959\,578^\circ$	$\delta = -21.312\,963^\circ$
$r_\alpha = -5.934\,39 \times 10^{-5}$	$r_\delta = 7.551\,66 \times 10^{-6}$	$\alpha = 238.817\,569^\circ$	$\delta = -21.300\,989^\circ$
$r_\alpha = 2.642\,89 \times 10^{-5}$	$r_\delta = 1.732\,93 \times 10^{-5}$	$\alpha = 238.742\,306^\circ$	$\delta = -21.221\,889^\circ$
$r_\alpha = -3.397\,78 \times 10^{-6}$	$r_\delta = 1.184\,61 \times 10^{-5}$	$\alpha = 238.798\,843^\circ$	$\delta = -21.162\,367^\circ$
$r_\alpha = 5.534\,77 \times 10^{-5}$	$r_\delta = -3.659\,27 \times 10^{-5}$	$\alpha = 238.864\,020^\circ$	$\delta = -21.150\,161^\circ$
$r_\alpha = -2.409\,74 \times 10^{-5}$	$r_\delta = 6.732\,73 \times 10^{-6}$	$\alpha = 238.896\,232^\circ$	$\delta = -21.190\,001^\circ$
$r_\alpha = -4.042\,72 \times 10^{-5}$	$r_\delta = 6.246\,76 \times 10^{-6}$	$\alpha = 238.990\,276^\circ$	$\delta = -21.127\,421^\circ$
$r_\alpha = -1.279\,44 \times 10^{-5}$	$r_\delta = -2.492\,73 \times 10^{-5}$	$\alpha = 238.820\,043^\circ$	$\delta = -21.333\,844^\circ$

Final α and δ fit

$$\alpha = 239.025\,973\,154 + -0.000\,577\,717\,223\,601x + 6.801\,177\,141\,39 \times 10^{-5}y$$
$$\delta = -21.111\,742\,027\,9 + -6.401\,418\,344\,86 \times 10^{-5}x + -0.000\,538\,501\,912\,862y$$

2014/07/22 04:38:34.12 UT (JD 2456861.693451)

$\boldsymbol{\alpha = 234.273581^h}$ $\boldsymbol{(15^h37^m5.66)}$	$c_x = 338.494$
$\boldsymbol{\delta = -23.294\,516^\circ}$ $\boldsymbol{(-23^\circ17'40.26'')}$	$c_y = 174.213$

Stars used in the least squares fit:

$r_\alpha = -2.217\,92 \times 10^{-5}$	$r_\delta = 3.795\,00 \times 10^{-5}$	$\alpha = 234.466\,107^\circ$	$\delta = -23.449\,266^\circ$
$r_\alpha = 1.703\,08 \times 10^{-4}$	$r_\delta = 4.469\,39 \times 10^{-5}$	$\alpha = 234.401\,369^\circ$	$\delta = -23.411\,539^\circ$
$r_\alpha = -9.454\,55 \times 10^{-5}$	$r_\delta = -2.086\,79 \times 10^{-5}$	$\alpha = 234.393\,271^\circ$	$\delta = -23.306\,613^\circ$
$r_\alpha = -1.317\,49 \times 10^{-5}$	$r_\delta = 4.693\,68 \times 10^{-5}$	$\alpha = 234.326\,081^\circ$	$\delta = -23.212\,078^\circ$
$r_\alpha = 5.321\,51 \times 10^{-5}$	$r_\delta = -6.739\,44 \times 10^{-7}$	$\alpha = 234.194\,448^\circ$	$\delta = -23.267\,471^\circ$
$r_\alpha = -4.738\,85 \times 10^{-5}$	$r_\delta = 3.515\,56 \times 10^{-5}$	$\alpha = 234.247\,680^\circ$	$\delta = -23.370\,668^\circ$
$r_\alpha = 2.881\,25 \times 10^{-5}$	$r_\delta = -4.364\,32 \times 10^{-5}$	$\alpha = 234.301\,660^\circ$	$\delta = -23.375\,412^\circ$
$r_\alpha = 3.112\,90 \times 10^{-5}$	$r_\delta = -5.459\,81 \times 10^{-5}$	$\alpha = 234.345\,162^\circ$	$\delta = -23.307\,749^\circ$
$r_\alpha = -9.156\,23 \times 10^{-6}$	$r_\delta = 3.148\,44 \times 10^{-5}$	$\alpha = 234.204\,789^\circ$	$\delta = -23.441\,861^\circ$
$r_\alpha = -9.702\,00 \times 10^{-5}$	$r_\delta = -7.643\,74 \times 10^{-5}$	$\alpha = 234.336\,598^\circ$	$\delta = -23.426\,410^\circ$

Final α and δ fit

$$\alpha = 234.468\,051\,732 + -0.000\,604\,637\,981\,164x + 5.852\,270\,756\,06 \times 10^{-5}y$$
$$\delta = -23.179\,421\,794\,8 + -5.419\,426\,579\,51 \times 10^{-5}x + -0.000\,555\,352\,750\,762y$$

Table 1: Table of observations

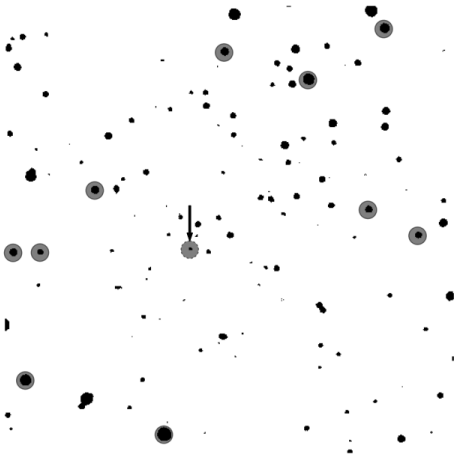

(a) 2014/06/27 06:39:41.31 UT

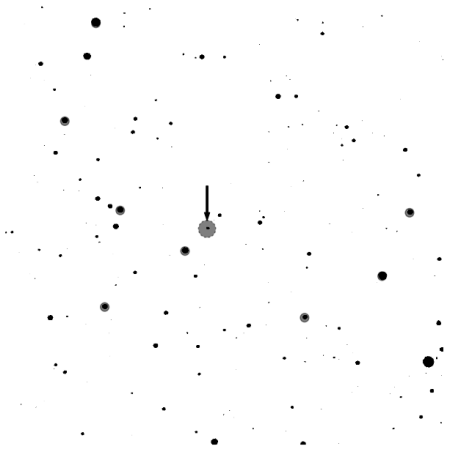

(b) 2014/07/02 07:13:55.00

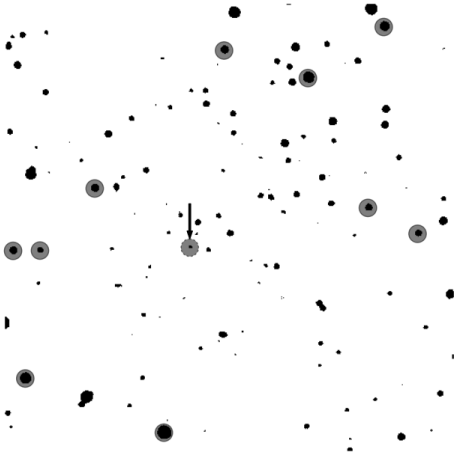

(c) 2014/07/05 06:53:11.59 UT

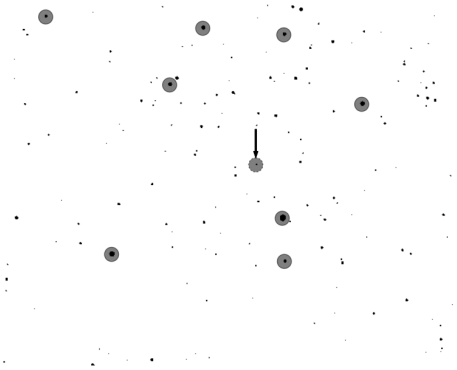

(d) 2014/07/11 06:46:41.38 UT

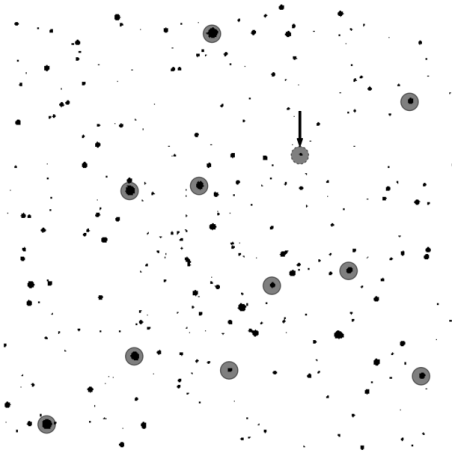

(e) 2014/07/22 04:38:34.12 UT

Figure 2: Images used during the orbit determination and the reference stars used in the least squares plate reduction.

	Calculated value	Horizons
a	2.9136 ± 0.2046	2.872004
e	0.7007 ± 0.0227	0.697078
i	$13.4179^\circ \pm 0.7980^\circ$	$13.334\,927^\circ$
Ω	$88.3553^\circ \pm 0.4534^\circ$	$88.396\,764^\circ$
ω	$275.9211^\circ \pm 1.4043^\circ$	275.7997°
T	2455122 ± 193	2455165.5532

Table 2: Calculated results compared to JPL Horizons accepted values. The calculated values come from the observations on June 27th, July 5th and July 11th (UT). Note that the Horizons values are those closest to current values (osculating elements).

Expected value	Observed value
2014/07/02 07:13:55.00 UT	
$\alpha = 16^h13^m35.9^s$	$\alpha = 16^h13^m36.52^s$
$\delta = -19^\circ47'41.2''$	$\delta = -19^\circ47'40.71''$
2014/07/22 04:38:34.12 UT:	
$\alpha = 15^h36^m55.7^s$	$\alpha = 15^h37^m5.66^s$
$\delta = -23^\circ17'19.5''$	$\delta = -23^\circ17'40.26''$

Table 3: Comparison between the expected (as predicted by the ephemeris generation program) right ascension and declination and the ones observed in the observations not used during the orbit determination. More details about these two observations can be found in table 1.

3.2. Orbital elements

Using the aforementioned methodology, five sets of measurable images were obtained. Of those, three of them were used to determine the orbit of the asteroid; the results can be found in Table 2. Note that they were compared against the osculating elements to account for the perturbed orbit of this asteroid.

3.3. Ephemeris check

Since we only used three out of five observations during the orbit determination, we can use the other two to perform an ephemeris check and compare our expected results to the actual results we could observe. These can be found in Table 3.

Using the aforementioned methodology, five sets of measurable images were obtained. Also used were four additional sets taken by the Omega Lobster team to get more accuracy.[10] The sets of images taken can be found in Figure 2 and the measurements of these in table 1.

3.4. Visualization

A visualization of the asteroid's orbit was made using Visual Python and can be found in Figure 3. Also included in Figure 4 is a visualization of the position of the asteroid and the Earth at the time of our three observations which we used during the orbit determination.

3.5. Orbit dynamics

Using numerical integration, close approaches to the Earth were determined by calculating the distance from the asteroid to the Earth. The closest approach within the next few years was calculated to be in November 17, 2014, at a distance of 0.135 AU. This value closely matches the

[10] Berger, Fang, and Khosla 2014.

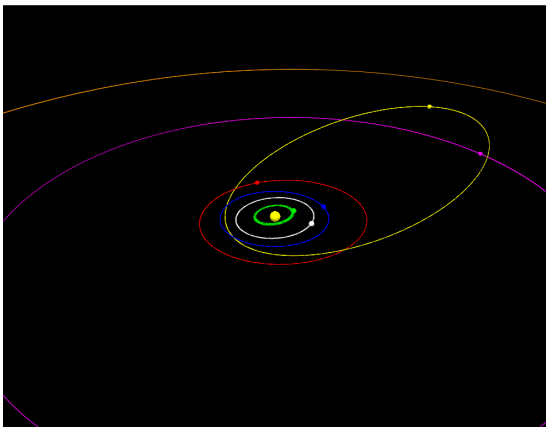

Figure 3: Visualization of the asteroid's orbit using Visual Python.

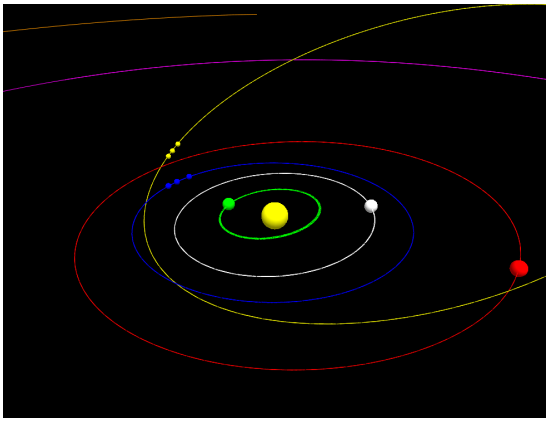

Figure 4: Positions of the Earth and the asteroid during each of the observations which we used to calculate the orbit.

one calculated by Pisa University in its Near Earth Objects page.[11]

The next close approach does not take place until five years later. However, the close approach at 0.135 AU suggests that further research on the long term dynamics of this asteroid should be done to assess potential risks. It must be taken into account that the numerical integration performed (while it does match current accepted data) does not take into account perturbations by other planets or other irregularities in the orbits.

4. Conclusion

The calculated classical orbital elements differ from the Horizons values. Although the values are within uncertainty, based on the ephemeris check, the calculated values appear to be more accurate than those found via the Horizons database. A potential explanation is that the orbit of the asteroid has been perturbed by another celestial body between the years 2009, which was when the Horizons elements were generated, and 2014, when the asteroid was measured. This implies that our data would be an improvement to the current JPL reported values.

The most effective way to improve the accuracy of our data is to determine a more accurate value for the distance between Earth and the asteroid. This can be accomplished by parallax, or the practice of measuring the asteroid from two different locations on the Earth to determine the difference in the apparent position of the asteroid. It is also possible to use radar to determine the distance to the asteroid, which would be much more precise. A precise value of ρ would be

[11] `http://newton.dm.unipi.it/neodys/index.php?pc=1.1.8&n=214088`

enough to calculate the vector elements of the asteroid by vector geometry. Another potential improvement is to use telescopes with larger mirror size to collect more light, which leads to a smaller uncertainty for the LSPR. These two improvements would be sufficient to further improve the clarity and accuracy of our images.

5. Acknowledgements

We would like to thank our peers, the Omega Lobster team of Mark Berger, Zhanpei Fang, and Kush Khosla for their amazing teamwork and for sharing their data, our phenomenal instructors, Dr. Michael Faison and Dr. Cassandra Fallscheer for teaching the Summer Science Program, as well as the teacher assistants Christine Chang, James Chang, Daksha Rajagopalan, and Andrew Warren for advice and encouragement. In addition, we thank Ms. Barbara Martinez for her tireless efforts in running the programm, Richard Bowdon, and the rest of the SSP trustees, board, and alumni for their generous support in making SSP a continuing reality.

References

Berger, Mark, Zhanpei Fang, and Kush Khosla (2014). "Orbit determination of 214088 (2004 JN 13)". In: *Summer Science Program 2014*.

Binz, Christopher R and Liam M Healy (2014). "Uncertainty Characterization for Angles-Only Initial Orbit Determination". In: *Advances in the Astronautical Sciences* 150, pp. 1777–1792.

Bisque, Software (2014). *TheSkyX Professional Edition*. URL: `http://www.bisque.com/sc/pages/TheSkyX-Professional-Edition.aspx`.

Danby, John (1992). "Fundamentals of celestial mechanics". In: *Richmond: Willman-Bell,— c1992, 2nd ed.* 1.

Gronchi, Giovanni F (2004). "Classical and modern orbit determination for asteroids". In: *Proceedings of the International Astronomical Union* 2004.IAUC196, pp. 293–303.

Hussein, Islam I et al. "PROBABILISTIC ADMISSIBILITY IN ANGLES-ONLY INITIAL ORBIT DETERMINATION". In:

JPL, NASA (2014). *625 Radar-Detected Asteroids and Comets*. URL: `http://echo.jpl.nasa.gov/asteroids/`.

Marsden, Brian G (1977). "Carl Friedrich Gauss, Astronomer". In: *Journal of the Royal Astronomical Society of Canada* 71, p. 309.

A. Method of Gauss

To evaluate the Method of Gauss, the following basic statements (as derived by Newton's Law of Gravitation) are used:

$$\mathbf{r} = \frac{-\mu \mathbf{r}}{r^3}$$

$$\hat{\mathbf{r}} = \rho\hat{\rho} - \hat{\mathbf{R}}$$

Next, we find some terms of the f and g series through the following formulas:

$$g = 1 - \frac{\tau^2}{2r^3} \cdots$$

$$f = \tau - \frac{\tau^3}{6r^3} \cdots$$

Afterwards, we calculate the constants a_1 and a_3 by:

$$a_1 = \frac{g_3}{f_1 g_3 - f_3 g_1}$$

$$a_3 = \frac{-g_1}{f_1 g_3 - f_3 g_1}$$

Using this, we are able to estimate the distance to the asteroid:

$$\rho_1 = \frac{\begin{array}{c} a_1(\mathbf{R}_1 \times \hat{\rho_2} \cdot \hat{\rho_3}) \\ -(\mathbf{R}_2 \times \hat{\rho_2} \cdot \hat{\rho_3}) + a_3(\mathbf{R}_3 \times \hat{\rho_2} \cdot \hat{\rho_3}) \end{array}}{a_1(\hat{\rho_1} \times \hat{\rho_2} \cdot \hat{\rho_3})}$$

$$\rho_2 = \frac{\begin{array}{c} a_1(\hat{\rho_1} \times \mathbf{R_2} \cdot \hat{\rho_3}) \\ -(\hat{\rho_2} \times \mathbf{R_2} \cdot \hat{\rho_3}) + a_3(\hat{\rho_3} \times \mathbf{R_2} \cdot \hat{\rho_3}) \end{array}}{a_1(\hat{\rho_1} \times \hat{\rho_2} \cdot \hat{\rho_3})}$$

$$\rho_3 = \frac{\begin{array}{c} a_1(\hat{\rho_2} \times \mathbf{R_1} \cdot \hat{\rho_1}) \\ -(\hat{\rho_2} \times \mathbf{R_2} \cdot \hat{\rho_1}) + a_3(\hat{\rho_2} \times \mathbf{R_3} \cdot \hat{\rho_1}) \end{array}}{a_1(\hat{\rho_1} \times \hat{\rho_2} \cdot \hat{\rho_3})}$$

Given these ρ values, we can determine the $\mathbf{r_2}$ and $||r_2||$ values, which is then reiterated above in the f and g series. This is continuously calculated until values begin to converge.

B. Orbital elements calculation

There are several equations used in the classical orbit element determinations. For full comprehension, these equations are summarized below:

Semi-major Axis:

$$\frac{1}{a} = \frac{2}{r} - \frac{v^2}{\mu}$$

Eccentricity:

$$e = \frac{\dot{\mathbf{r_0}} \times \mathbf{h}}{\mu} - \hat{r_0}$$

Inclination:

$$i = \arccos(\frac{\mathbf{h} \cdot \hat{\mathbf{z}}}{h})$$

Longitude of Ascending Node:

$$\Omega = \arccos(\frac{\mathbf{N} \cdot \hat{\mathbf{x}}}{N})$$

Argument of Perihelion:

$$\omega = \arccos(\frac{\mathbf{N} \cdot \mathbf{e}}{N \cdot e})$$

Ascending Node:

$$N = \hat{\mathbf{z}} \times \mathbf{h}$$

Mean Anomaly:

$$M = k\sqrt{\frac{\mu}{a^3}}(t - T)$$

$$M = E - e \sin E$$